

Surface electronic structure of Sr_2RuO_4

K. M. Shen, A. Damascelli, D. H. Lu, N. P. Armitage, F. Ronning, D. L. Feng, C. Kim, and Z.-X. Shen
Department of Applied Physics, Physics, and Stanford Synchrotron Radiation Laboratory, Stanford University, Stanford, California 94305

D. J. Singh and I. I. Mazin
Naval Research Laboratory, Code 6391, Washington, D.C. 20375

S. Nakatsuji, Z. Q. Mao, and Y. Maeno
*Department of Physics, Kyoto University, Kyoto 606-8502, Japan
 and CREST-JST, Kawagushi, Saitama 332-0012, Japan*

T. Kimura and Y. Tokura
*Department of Applied Physics, University of Tokyo, Tokyo 113-8656, Japan
 and JRCAT, Tsukuba, 305-0046, Japan*

(Received 24 May 2001; published 2 October 2001)

We have addressed the possibility of surface ferromagnetism in Sr_2RuO_4 by investigating its surface electronic states by angle-resolved photoemission spectroscopy (ARPES). By cleaving samples under different conditions and using various photon energies, we have isolated the surface from the bulk states. A comparison with band structure calculations indicates that the ARPES data are most readily explained by a *nonmagnetic* $\sqrt{2} \times \sqrt{2}$ surface reconstruction.

DOI: 10.1103/PhysRevB.64.180502

PACS number(s): 74.70.Pq, 74.25.Jb, 73.20.At

Following the discovery of superconductivity (SC) at 1 K in the layered perovskite Sr_2RuO_4 ,¹ the exact nature of its SC pairing mechanism has attracted a great deal of interest. While it shares the same structure as the archetypal cuprate parent compound La_2CuO_4 , RuO_2 planes replace the CuO_2 planes thus resulting in an anisotropic Fermi liquid² instead of a strongly correlated charge transfer insulator. Furthermore, there is evidence that Sr_2RuO_4 exhibits spin-triplet pairing with a *p*-wave order parameter,³ as opposed to the spin-singlet, *d*-wave symmetry found in the cuprates. Although it is now widely believed that the unconventional nature of SC in this compound is mediated by spin fluctuations, the exact nature of this interaction is still unresolved. Originally, it was suggested that ferromagnetic (FM) spin fluctuations were responsible for mediating the SC as inferred from theoretical calculations,⁴ NMR measurements,⁵ and ferromagnetism in closely related SrRuO_3 . However, more recent evidence has suggested that this simple picture may be incomplete. Antiferromagnetism (AFM) in Ca_2RuO_4 , the observation of incommensurate peaks at $\mathbf{Q} = (0.6\pi, 0.6\pi, 0)$ by neutron scattering,⁶ and calculations which show strong nesting at $\mathbf{Q} = (2\pi/3, 2\pi/3, 0)$ (Ref. 7) all seem to imply that AFM correlations should not be neglected, leaving the nature of SC open to speculation.

Recently, an analysis of low-energy electron diffraction data from Sr_2RuO_4 indicated that a $\sqrt{2} \times \sqrt{2}$ reconstruction was induced by the freezing of a soft zone boundary phonon into a static lattice distortion at the surface, and comparisons with band structure calculations predicted that the resulting surface was FM.⁸ This possibility was also speculated upon in a recent angle-resolved photoemission spectroscopy (ARPES) study by our group,⁹ as well as in earlier theoretical calculations.¹⁰ If FM does exist on the surface of Sr_2RuO_4 , such a result should be indicative of strong ferro-

magnetic tendencies in the bulk and thus possibly relevant to microscopic theories which describe the mechanism of SC. This speculation becomes even more intriguing in light of recent scanning tunneling microscopy measurements¹¹ which suggest the opening of a superconducting gap with $T_c = 1.4$ K, perhaps hinting that the surface layer may be superconducting, and raises the possibility that the surface of Sr_2RuO_4 may exhibit the rare coexistence of SC and FM. However, as this proposed surface FM has never been confirmed, it becomes imperative to reinvestigate the *surface* electronic structure to definitively verify or exclude surface FM.

In this paper, we present a detailed, high-resolution ARPES study of the surface electronic structure of Sr_2RuO_4 . While our earlier work⁹ ascertained that the *bulk* Fermi surface (FS) topology extracted by ARPES was indeed in excellent agreement with both theory^{12,13} and de Haas-van Alphen (dHvA) results,² the precise nature of the surface-derived states, which could be nonmagnetic (NM) or FM, remained ambiguous. In particular, our earlier depiction of the surface electronic structure failed to explicate the presence of the intense, surface-derived peak at $(\pi, 0)$, leaving us to speculate that its existence could be a possible manifestation of surface FM. To clarify this uncertainty, we have performed a comprehensive ARPES study with various photon energies and polarizations in conjunction with detailed band structure calculations which now account for the surface reconstruction. By comparing these calculations with our ARPES data, we conclude that our results are consistent with the NM scenario and exhibit no experimentally detectable trace of surface FM down to 10 K.

ARPES data were taken at the Stanford Synchrotron Radiation Laboratory using a Scienta SES-200 analyzer with typical resolutions of $\Delta E < 13$ meV and $\Delta \theta \approx 0.2^\circ$.

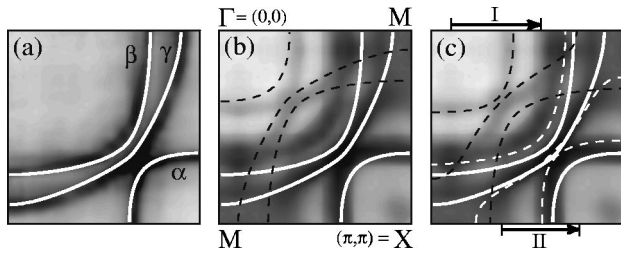


FIG. 1. (a) E_F intensity map of Sr_2RuO_4 cleaved at 180 K and measured at 10 K with $h\nu=28$ eV and overlaid theoretical FS's. (b) and (c) show an intensity map from a sample cleaved and measured at 10 K. (b) shows calculated bulk FS's (white) with trivial folded FS's (dashed), while (c) shows calculated 6° NM reconstruction with both primary and folded surface FS's (dashed white and dashed black).

Sr_2RuO_4 single crystals were first aligned by Laue diffraction and then cleaved *in situ* at a pressure of better than 5×10^{-11} torr and at various temperatures described below. All spectra were measured at 10 K in both the first and second Brillouin zones; surface features showed slight enhancement in the second zone.

Figure 1(a) shows an E_F intensity map (integrated signal within $E_F \pm 5$ meV) of a sample cleaved at 180 K and measured at 10 K. As discussed in Ref. 9, cleaving the sample at elevated temperatures preferentially suppresses the surface intensity; we speculate that the increased rate of thermally activated oxygen diffusion results in a more disordered surface layer. The resulting intensity map thereby primarily reflects the bulk contribution, and the calculated bulk FS's from Ref. 13 are overlaid and in excellent agreement. When cleaving at lower temperatures, the surface states were well preserved and also apparent in our data, in addition to the bulk states. This additional surface contribution is clearly visible in the intensity maps in Figs. 1(b) and 1(c) and somewhat complicates the situation. Our original conjecture, in Ref. 9 and shown in Fig. 1(b), accounted for the surface states by considering them to be the same as those of the bulk, except for a rigid folding due to the $\sqrt{2} \times \sqrt{2}$ surface reconstruction; the reconstruction arises from rotations of the RuO_6 surface octahedra which cause a doubling of the surface unit cell.⁸ Despite the approximate agreement, this overly simplistic picture fails to explain the origin of the strong peak [bottom of Fig. 2(b)] at M, which influenced earlier ARPES reports to erroneously designate the bulk γ -FS as holelike.^{14,15} This apparent discrepancy also led us to initially posit that surface FM might be responsible for this state at M. However, after calculating the precise effects of the surface distortion on the band structure, we find that the NM reconstruction alone can potentially drive the surface γ -FS holelike, thus explaining the peak at M; this more accurate NM scenario is depicted in Fig. 1(c).

Nonetheless, since surface FM might still account for some of the experimentally observed features, it becomes crucial to examine the surface states in greater detail. In particular, surface FM would cause the surface states to split into minority and majority bands, effectively doubling the number of surface-derived bands. In order to distinguish be-

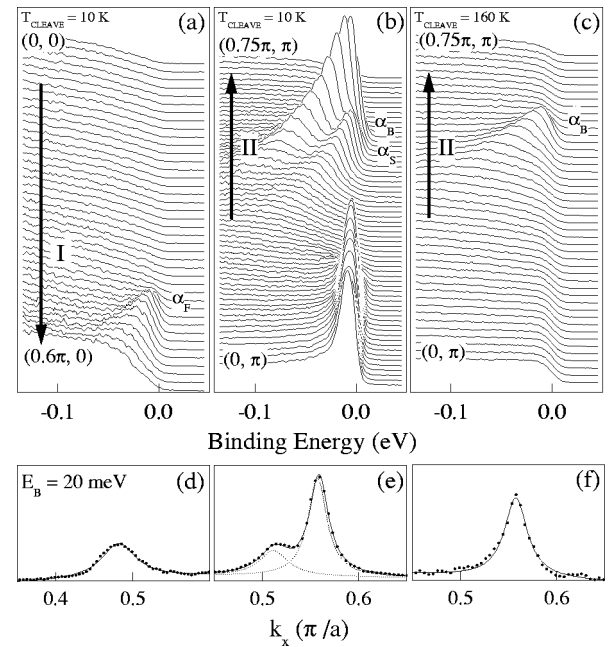


FIG. 2. EDC's in panels (a), (b), and (c) taken along cuts I and II shown in Fig. 1. Corresponding MDC's at $E_B=20$ meV taken from (a), (b), and (c) are shown in panels (d), (e), and (f), respectively. Data from (a), (b), (d), and (e) were taken on a sample cleaved at 10 K, while data from (c) and (f) were taken on a sample cleaved at 160 K. α_F , α_S , and α_B refer to folded, surface, and bulk α bands, respectively.

tween the NM and FM scenarios, we focus on ARPES spectra taken along lines I and II in Fig. 1(c). For the NM surface, we would expect to see one band, α_F , crossing along I and two crossings, α_S and α_B , along II. Any additional bands beyond those predicted for the NM surface would be strong evidence for surface FM, and should be readily apparent in the ARPES data.

To address this issue, we first focus on spectra taken along I, shown in Fig. 2(a), using 24 eV photons polarized along the Ru-O bond direction; different photon energies and polarizations yielded similar results. This region is particularly suitable for an investigation into potential surface FM since it is far removed from the bulk electronic states. Examining the energy distribution curves (EDC's) in Fig. 2(a), we see only a single electronic state from the folded α -FS, denoted as α_F , as is expected from the NM scenario shown in Fig. 1(c). Conversely, additional bands reflecting the exchange splitting would be expected for a FM surface. In Fig. 2(d), we show a momentum distribution curve (MDC) of data from Fig 2(a), where the photoemitted electron intensity is displayed as a function of momentum at a fixed binding energy of $E_B=20$ meV and fitted to a single Lorentzian line shape on a linear background. By analyzing our data in this fashion, we are able to track the dispersion of α_F yielding $v_F^F=0.7$ eV \AA . Therefore our measurements along I yield only a single surface band, consistent with the nonmagnetic scenario of Fig. 1(c).

To further reinforce this result, we now consider data along II shown in Fig. 2(b), taken under the same conditions as I, but in the second zone. In both the EDC's and MDC's,

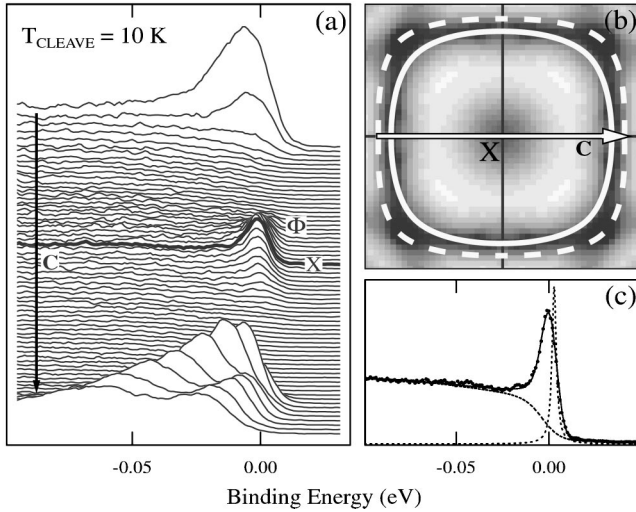


FIG. 3. ARPES data taken near X with $h\nu=24$ eV at 10 K on a sample cleaved 10 K. EDC's in (a) were taken along cut C. (b) shows an E_F intensity map (± 5 meV) around the region of the bulk and surface α -FS's, shown in solid and dashed white, respectively. (c) shows the EDC from X and the corresponding fit. The background curve and the Lorentzian used in fitting are also shown as dotted lines.

one can clearly observe two distinct peaks. By fitting the MDC's to a double-Lorentzian form, shown in Fig. 2(e), and tracking their dispersion to E_F , one can determine the Fermi velocities of the two bands. From this analysis, we determine the velocity of the first band, α_B , to be $v_F^B=1.1$ eV \AA , while for the second, α_S , $v_F^S=0.7$ eV \AA . On another sample cleaved at 160 K with the measurement taken in otherwise identical conditions, α_S is suppressed, as shown in Fig. 2(c), and the remaining state is the bulk-derived α_B ; both α_B features in Figs. 2(b) and 2(c) have the same v_F and Fermi crossing position. Also note that cleaving at elevated temperatures completely suppresses the strong peak at the bottom of Fig. 2(b), which is also responsible for the weight at M in Figs. 1(b) and 1(c). Furthermore, we are able to conclude that α_F is simply the folded counterpart of the surface-derived α_S , and not the counterpart of the bulk-derived α_B , since α_S and α_F have matching v_F and Fermi crossings in the reduced zone. Therefore, the absence of additional bands along Π is consistent with our results from I and our conclusion of a NM surface.

Examining EDC's taken over the entire zone, virtually all observed surface states can be well accounted for by considering only a NM surface. The only unexpected feature was a small peak localized around X, hereafter denoted as Φ , as shown in Figs. 3(a) and 3(b), which was most strongly enhanced at $h\nu=24$ eV. Close inspection of the spectrum at X in Fig. 3(c) reveals that the peak position is located at E_F (± 1 meV) and the leading edge is 6 meV above E_F , indicating that this peak originates from above E_F ; the peak in the EDC's is the product of the rising tail of the quasiparticle peak and the falling edge of the Fermi-Dirac function. This was confirmed by fitting the data using a background taken from $(0.8\pi, \pi)$ and a Lorentzian peak, both multiplied by a Fermi-Dirac function and convolved with our resolution

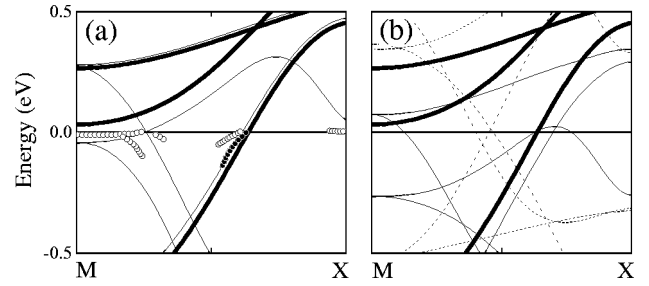


FIG. 4. (a) Band structure calculations along M-X for bulk and 6° NM surface (thick and thin lines) along with ARPES dispersion for bulk and surface states (solid and open circles). (b) Bulk, minority surface, and majority surface bands in thick, thin, and dashed lines for a 6° FM surface.

($\Delta E=8$ meV), allowing us to estimate a peak position of 3 meV above E_F and an intrinsic full width at half maximum of 3 meV. Although there may be some slight inaccuracies in the fitting procedure, all attempts to fit the spectra to a below- E_F peak proved wholly unsuccessful. Moreover, since no corresponding band can be seen to disperse from below E_F , we can conclude that Φ arises from an unoccupied band whose minimum at X almost grazes E_F . Naively, one might infer that this somewhat unexpected feature could be interpreted as evidence for surface FM. However, as will be discussed below, our calculations, in fact, even predict the appearance of Φ , which arises from the distortion of the surface layer.

In order to gain deeper insight into the effects of the surface reconstruction, we have performed both NM and FM calculations similar to those reported in Ref. 13, but including rotations by a fixed angle in all RuO₂ planes, resulting in a monoclinic $C2/m$ symmetry. We will hereafter refer to these rotated bulk calculations as pertaining to the surface, and this assumption can be justified because of the extremely two-dimensional nature of the electronic structure; any effects from the surface termination should be far weaker than those of the rotations of the octahedra, and this is demonstrated by the excellent agreement of our NM rotated calculations with the corresponding surface calculations performed by Fang.^{8,16}

Figure 4(a) shows the results of NM calculations along the tetragonal M-X direction for rotations of $\theta=0^\circ$ (bulk) and $\theta=6^\circ$ (NM surface). An angle of 6° was chosen since it is within the error bars of the structural data⁸ and also gives good agreement with our ARPES data, especially the placement of Φ . The NM surface and bulk bands are shown in Fig. 4(a), and the experimentally determined values are overlaid and in good agreement with theory.¹⁷ We also note that our estimate of the quasiparticle renormalization $v_F^{calc}/v_F^B=3.2$ for the bulk α -FS along M-X is in excellent agreement with $m^*/m_{band}=3.3$ from dHvA,² and also close to theoretical estimates of ≈ 2.5 .¹⁸ Calculations for $\theta=6^\circ$ produce the dashed FS's in Fig. 1(c) and the rotation induces various effects.

First, the extended van Hove singularity (evHs) at M, which is 60 meV above E_F in the bulk calculations, is pushed 40 meV below E_F due to the repulsion between the

d_{xy} and $d_{3z^2-r^2}$ bands, which is allowed only in the lowered symmetry of the distorted surface. This results in the topology of the surface γ -FS changed from electronlike to holelike, as shown in Fig. 1(c), also concurring with independent calculations from Ref. 19. Furthermore, the dispersion of this feature, in agreement with Refs. 14 and 15, is consistent with the saddlepoint topology predicted by theory.

Secondly, the lower symmetry on the surface also allows for hybridization between the d_{xy} and $d_{x^2-y^2}$ bands forbidden in the tetragonal symmetry. In the distorted structure, these two states are both at the now-equivalent Γ/X point of the downfolded zone and repel each other. Furthermore, rotations disrupt the Ru-O $pd\sigma$ hopping more strongly than the $pd\pi$ hopping and thus the $d_{x^2-y^2}$ band moves down relative to the d_{xy} band. Both effects together lead to the formation of a strongly mixed state at the Γ/X point which moves down rapidly and gains more $d_{x^2-y^2}$ character with rotation angle. While it is 300 meV above E_F for $\theta=0^\circ$, it crosses E_F for $\theta=7^\circ$, and is the origin of Φ . Although Φ was not observed at Γ , this absence is not surprising when considering the unfavorable photoemission matrix elements due to the significant $d_{x^2-y^2}$ and d_{xy} character of this state.

The effects of FM on the surface electronic structure were evaluated by performing constrained fixed spin moment calculations for the 6° surface with an imposed magnetization of $1\mu_B/\text{Ru}$, a value consistent with Ref. 8. The corresponding FM surface calculation is shown in Fig. 4(b) and is radically different from what is measured experimentally; for instance, both the evHs at M and the bottom of the $d_{xy}/d_{x^2-y^2}$ band at X are absent. Regardless of the particular details of the calculations, such as the position of the chemical potential and the bands, even the number of bands expected and measured are in disagreement, thus favoring the NM scenario, in contrast to the earlier speculation by our group⁹ and Matzdorf *et al.*⁸

Although exact comparisons between the theoretical calculations and the ARPES data can be somewhat difficult due to the significant electron-electron interactions, the qualita-

tive comparison of the ARPES data with the general behavior of the calculated electronic structure should be robust. The earlier conclusion of surface FM (Ref. 8) was based on the comparison of structural data ($\theta=9^\circ\pm 3^\circ$) to magnetic band structure calculations. However, the error bars in the structural data are comparable to the spread in the calculated rotation angles for a NM (6.5°), AFM (6.5°), and FM surface (9°), leaving room open for alternative interpretations of the data. Furthermore, the generalized gradient approximation employed in the aforementioned calculations may be inclined to overestimate the tendency towards magnetism, and even incorrectly predicts ferromagnetism in bulk Sr_2RuO_4 .¹⁰ We can place a maximum upper bound on the strength of any existing FM by considering our experimental resolution and the width of the quasiparticle peaks. If we assume that both α_S and α_F were comprised of a pair of extremely weakly split FM bands, we are able to put an upper bound of $E_{exch}\approx 15$ meV, which is much smaller than the predicted FM exchange splitting of ≈ 500 meV.^{10,16} Using this value of $E_{exch}\approx 15$ meV results in an upper bound for the spin polarization of $<0.05\mu_B/\text{Ru}$, much weaker than predicted theoretically.

In conclusion, we have isolated and directly studied the surface-derived electronic states in Sr_2RuO_4 by ARPES. By comparison with detailed band structure calculations, we find that the origin of the ARPES features can be simply explained by considering the effect of a nonmagnetic surface reconstruction on the electronic structure, with no evidence of surface FM.

We thank Z. Fang and K. Terakura for kindly discussing their unpublished band structure calculations with us. K.S. acknowledges SGF and NSERC for their support. The work at NRL was supported by the ONR. SSRL is operated by the DOE Office of Basic Energy Research, Division of Chemical Sciences. The office's division of Material Science provided support for this research. The work at Stanford University was also supported by NSF Grant No. DMR9705210 and ONR Grant No. N00014-98-1-0195.

¹Y. Maeno *et al.*, Nature (London) **372**, 532 (1994).

²A.P. Mackenzie *et al.*, Phys. Rev. Lett. **76**, 3786 (1996).

³K. Ishida *et al.*, Nature (London) **396**, 658 (1998).

⁴I.I. Mazin and D.J. Singh, Phys. Rev. Lett. **82**, 4324 (1999).

⁵T. Imai *et al.*, Phys. Rev. Lett. **81**, 3006 (1998).

⁶Y. Sidis *et al.*, Phys. Rev. Lett. **83**, 3320 (1999).

⁷I.I. Mazin and D.J. Singh, Phys. Rev. Lett. **82**, 4324 (1999).

⁸R. Matzdorf *et al.*, Science **289**, 746 (2000).

⁹A. Damascelli *et al.*, Phys. Rev. Lett. **85**, 5194 (2000).

¹⁰P.K. de Boer and R.A. de Groot, Phys. Rev. B **59**, 9894 (1999).

¹¹A. Morpurgo (private communication).

¹²T. Oguchi, Phys. Rev. B **51**, 1385 (1995).

¹³D.J. Singh, Phys. Rev. B **52**, 1358 (1995).

¹⁴T. Yokoya *et al.*, Phys. Rev. B **54**, 13 311 (1996).

¹⁵D.H. Lu *et al.*, Phys. Rev. Lett. **76**, 4845 (1996).

¹⁶Z. Fang (private communication).

¹⁷ v_F^B/v_F^S is larger than calculated. This may be due to the relaxation of the apical oxygen, additional tilting of the RuO_6 octahedra, or even different electron-phonon coupling at the surface, but does not change our arguments.

¹⁸A. Liebsch and A. Lichtenstein, Phys. Rev. Lett. **84**, 1591 (2000).

¹⁹A. Liebsch (private communication).